JOURNAL OF VIROLOGY, Aug. 1988, p. 2960–2969
0022-538X/88/082960-10$02.00/0

Vol. 62, No. 8

Length and Shape Variants of the Bacteriophage T4 Head: Mutations in the Scaffolding Core Genes 68 and 22

BEAT KELLER,[1]† JACQUES DUBOCHET,[2]‡ MARC ADRIAN,[2]§ MARLIES MAEDER,[1] MICHEL WURTZ,[1] AND EDWARD KELLENBERGER[1]*

Department of Microbiology, Biozentrum, Universität Basel, Klingelbergstrasse 70, CH-4056 Basel, Switzerland,[1] and European Molecular Biology Laboratory, D-6900 Heidelberg, Federal Republic of Germany[2]

Received 11 December 1987/Accepted 23 April 1988

The shape and size of the bacteriophage T4 head are dependent on genes that determine the scaffolding core and the shell of the prohead. Mutants of the shell proteins affect mainly the head length. Two recently identified genes (genes 67 and 68) and one already known gene (gene 22), whose products are scaffold constituents, have been investigated. Different types of mutants were shown to strongly influence the proportion of aberrantly shaped particles. By model building, these shape variants could be represented as polyhedral bodies derived from icosahedra, through outgrowths along different polyhedral axes. The normal, prolate particle is obtained by elongation along a fivefold axis. The mutations of the three core genes (genes 67, 68, and 22) affect the width mainly by lateral outgrowths of the prolate particle, although small and large isometric particles are also found. Many of the aberrant particles are multitailed, suggesting a correlation between tail attachment sites and shape.

The formation of the heads of bacterial viruses proceeds through a complex series of assembly and maturation steps. This morphogenesis is based only on mechanisms involving protein-protein and protein-nucleic acid interactions and is not under transcriptional control (15). In bacteriophage T4 infections, a prohead is initially bound to the bacterial membrane. This prohead is matured by proteolytic cleavage (37) of all but one of its protein constitutents, expanded, and filled with DNA (for a review, see reference 4).

The prohead consists of a proteinaceous scaffolding core (13, 36) which is surrounded by a shell. The scaffolding core is made of at least seven protein species (31, 35); the shell is made of only two. The prohead already has a fully determined size and shape (12). The prolate (elongated) shape of the future normal head is also found in the naked scaffolding core when the shell protein is missing (36). Mutants with mutations in both shell proteins (9, 12) and scaffolding core proteins (20, 21, 29) give form variants of mature phages reflected either only in the length or in both the length and the overall shape (3, 28). The mechanism of length determination is not known. Several models have been suggested, among them the kinetic model which proposes that the length of the T4 head depends on the rate of growth of the core versus that of the shell (32). The experiments of Traub and Maeder (36), however, suggested that the scaffolding core alone controls the prohead shape. In their model the shell assembles passively around the core, either concomitantly or lagging behind; the intrinsic curvature of the shell complies with the core diameter.

To understand the structure of the T4 head and the mechanism of the prohead assembly, wild-type phage, as well as mutants of all known shell and core proteins, have been studied (4, 21). The mature T4 head was found to be an elongated icosahedron (for a review, see reference 10). The consequences of mutations in genes coding for core and shell proteins on head form were studied mainly by observing the final phage, which is easily accessible and less fragile than the prohead. In this report we describe several mutants in genes 68 and 22 and their effect on phage production. Aberrantly shaped heads were studied by electron microscopy, using preparation methods which optimally preserve the form of the phage head.

MATERIALS AND METHODS

Bacteria, bacteriophages, and plasmids. The standard hosts for bacteriophage T4 were *Escherichia coli* B and CR63 (*supD*) (14). For plasmid work we used strain WA803 (r_K^- m_K^- *met gal lac supE*) from the collection of W. Arber. All bacteriophages were derivatives of T4D$^+$ and were from the Basel collection. The T4 21*ts*E322 mutant was a temperature-sensitive (*ts*) derivative of T4 21*am*E322. Recombinant plasmids containing T4 DNA were pTV44 (38) and pBK21 (21). M13mp8, M13mp9, M13mp10, and M13mp11 (25) were from C. Sengstag of our laboratory. The bacteria were grown in M9 medium (1) supplemented with 1% Casamino Acids (M9A).

In vitro mutagenesis of gene 68. The construction of 68*fs*xho was described earlier (21). The deletion 68*del*a was made by opening pBK21 containing gene 67 and gene 68 with *Xho*I and digesting it with *Bal*31 nuclease by the method of Maniatis et al. (24). For this reaction, we used 12.5 μg of DNA in 100 μl at 30°C. At different times the reaction was stopped. Aliquots were analyzed by gel electrophoresis to identify the sample with the appropriate deletion upstream of the *Xho*I site. To this sample, 1.75 μg of unphosphorylated *Bam*HI linker d(CGGGATCCCG) (Boehringer GmbH) was added in 25 μl and ligated. The DNA was heated to 68°C for 5 min, and noncovalently bound linkers were separated from the plasmid DNA by electrophoresis and ligated after isolation from the gel. Following transformation, single colonies were grown up and plasmids were analyzed by digestion with *Bam*HI and separation on a 4% acrylamide gel. Appro-

* Corresponding author.
† Present address: The Salk Institute, San Diego, CA 92138.
‡ Present address: Centre de microscopie électronique CME, CH-1005 Lausanne, Switzerland.
§ Present address: European Molecular Biology Laboratory Outstation at the ILL, F-38041 Grenoble Cédex, France.

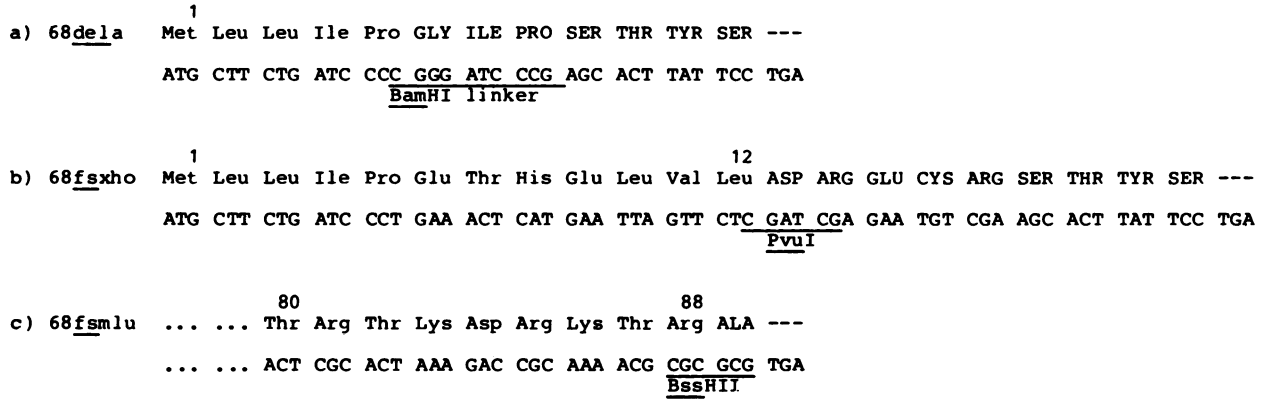

FIG. 1. DNA and amino acid sequence of mutants in gene 68. (a) 68*dela* (b) 68*fs*xho (c) 68*fs*mlu. The numbers of amino acids in the protein fragment are indicated. Capital letters emphasize amino acids in the protein fragments which are altered owing to the frame shift.

priate clones were chosen, and the *Bam*HI fragment containing gene 68 was cloned in M13mp8 (25) and sequenced by the chain termination method (30). A clone having only a small deletion downstream of the *Xho*I site was also isolated and cut with *Bam*HI, and the largest fragment was purified and ligated with the *Bam*HI fragment (containing gene 67 and the beginning of gene 68) of a clone having a useful deletion upstream of the *Xho*I site. A clone with the correct orientation was digested with *Sac*I, and the 1.1-kilobase-pair fragment was cloned into the *Sac*I site of pTV44. From this plasmid the mutation was recombined back to the T4 genome as described previously (21). The DNA sequence of 68 *dela* compared with that of the wild-type gene is shown in Fig. 1. Plasmid 68*fs*mlu was constructed by cleaving pTV44 at its unique *Mlu*I site in gene 68, filling the protrusive ends with Klenow polymerase, and religating as described for the 68*fs*xho mutation. Before transformation with the resulting ligation mixture, it was cleaved again with *Mlu*I to linearize the nonreacted molecules. Plasmids from transformed cells were checked for the presence of a new *Bss*HII restriction site created by the procedure. The frame-shifted gene was then recombined back to the T4 genome as we described previously (21). The structure of 68*fs*mlu is also given in Fig. 1. Neither mutant produced any protein detectable on immunoblots after reaction with anti-gp68 sera (results not shown).

Electron microscopy. Phages were prepared for electron microscopy by two different methods. For negative staining a drop of the sample was adsorbed to glow-discharged carbon-coated collodion films on copper grids and then stained. For better preservation, we used the procedure described by Doerman et al. (9): the adhering phages were rinsed with TAM (10 mM Tris, 1 mM Mg^{2+}, 10 mM NaN_3 [pH 7]) or H_2O (to remove PO_4^{3-}) and then soaked for 30 min in saturated uranyl acetate for cross-linking the DNA; the specimen was then air dried from 1% uranyl acetate. For electron microscopy of frozen-hydrated (vitrified) specimens the samples were prepared as described by Adrian et al. (2): a thin film of bacteriophage suspension was prepared by blotting away most of a drop applied to a perforated carbon film and projected into liquid nitrogen cooled ethane for vitrification. The samples were transferred into liquid nitrogen and from there into the cryo-specimen holder (PW 6591/100) of a Philips 400 electron microscope, where they were observed at a low dose (less than 2,000 electrons per nm^2) at −160°C. For conventional thin sections of phage-infected cells the bacterial culture was fixed in a mixture of glutaraldehyde and acrolein (36). Cells were infected at a multiplicity of infection of 5 and superinfected 6 min later with the same number of phages. Micrographs were taken with a Philips 300 electron microscope on Agfa-Gevaert HDU film at 80 kV.

Gel electrophoresis and immunoblotting. Sodium dodecyl sulfate-polyacrylamide gel electrophoresis was performed as described by Laemmli (23). Proteins were blotted from polyacrylamide gels to nitrocellulose by the method of Towbin et al. (34), the blots were treated with antibodies, and the cross-reacting bands were detected as described by De Blas and Cherwinski (8) with antibody-coupled peroxidase.

Construction of double mutants. The construction of the 67*am*K1 · 68*fs*xho double mutant has been described previously (20). Mutants 23*am*H11 · 68*fs*xho and 23*am*H11 · 68*fs*mlu were constructed by recombination between plasmid pTV44 with the 68*fs*xho or 68*fs*mlu frameshift mutations, respectively, and infecting phage mutant 20*ts*A3 · 21*ts*E322 · 23*am*H11. Phages growing at 42°C on *E. coli* CR63 were checked for production of gp68 by immunoblotting.

The two mutations 21*ts*N8 and 68*fs*xho were first combined on a plasmid. From pTV44-68*fs*xho the large *Mlu*I-*Pvu*II fragment containing part of gene 20, gene 67, and part of gene 68 (21) (Fig. 1) was isolated. This fragment was ligated with a *Mlu*I-*Pvu*II fragment containing part of gene 68, gene 21 with the 21*ts*N8 mutation (18), and part of gene 22. The two mutations were rescued from the plasmid by infecting the host with a 20*am*N50 · 21*am*H29 double mutant. Rescued phages grown on *E. coli* B at 30°C were first tested for the 21*ts*N8 mutation by the complementation test. The absence of gp68 was checked by immunoblotting.

Model construction of the different T4 head shapes. The principles of icosahedral symmetry and quasiequivalence and the basis of model construction have been described by Caspar and Klug (7). The regular head surface is folded from a two-dimensional hexagonal plane net (*p*6 net) on which the asymmetric protein subunits are positioned. Paper models of the different shape variants are obtained by folding and removing sectors (generally 60°) from this *p*6 net. The models have to fulfill the strict requirement that the surface pattern shows no discontinuity even at places where cutting edges are joined together. Vertices then occur automatically as coordinated groups of five protomers (pentamers), while elsewhere on the facets, only coordinated groups of six promoters (hexamers) are present. The basic *p*6 net is

TABLE 1. Burst size of gp68 mutant-infected cells compared with the wild type

Mutant	% of wild type burst size	No. of expt
68*dela*	24% ± 6%	2
68*fs*xho	15% ± 5%	3
68*fs*mlu	28% ± 5%	3

triangulated; each unit equilateral triangle contains three protomers; two such triangles constitute the unit cell. The isometric (regular) icosahedron is composed of $n = 20$ facets made of equilateral triangles, each containing T small unit triangles. T is called the triangulation number (7). The total number of subunits on the surface of this regular icosahedron is then $20 \times 3 \times T = 60T$. Any polyhedral body which derives from this icosahedron is constituted by an ensemble of equilateral and of irregular triangles. Their size is defined by their triangulation number, T, for equilateral faces or, by analogy, Q if the face is an irregular triangle, and the number of protomers, S, per triangle is again $3T$ or $3Q$.

The icosahedron-derived polyhedra are now easily described by the number of triangles of a given type, n_T or n_Q. The number of subunits (S) is then

$$S = 3 \sum_{T,Q} (n_T T + n_Q Q)$$

where $n_T + n_Q = 20$, or, written differently,

$$S = 60 \sum_{T,Q} \left(\frac{n_T}{20} T + \frac{n_Q}{20} Q \right)$$

where $n_T/20$ or $n_Q/20$ are the relative numbers of triangles of either type (T or Q). From these formulas the particular cases of regular or prolate icosahedra are easily derived (see Table 4).

TABLE 2. Morphology of mature phages[a]

Particle class	% of particles in class for following mutants:			
	68*dela*	68*fs*xho	68*fs*mlu	T4D$^+$
Prolate	39	48	69	99
Isometric	53	48	27	1
Biprolate with one or two tails	8	4	4	

[a] 300 particles were counted for each mutant. Phage lysates were prepared by infection of liquid cultures of *E. coli* B at a density of 2×10^8 cells/ml at a multiplicity of infection of 5 and superinfection 6 min later. The infected culture was further grown at 37°C for 60 min and then harvested and lysed with chloroform.

RESULTS

Mutations in gene 68. The three frameshift and deletion mutations in gene 68 are shown in Fig. 1. The predicted protein fragments produced have lengths of 12, 21, and 89 amino acid residues, of which the first 5, 12, and 88, respectively, correspond to the wild-type sequence. The predicted native wild-type protein is 141 amino acids long, of which the first 16 amino acids are cleaved off during head maturation. Plasmid 68*dela* produces the shortest fragment, of 12 amino acids (Fig. 1a). In plasmid 68*fs*xho (Fig. 1b) a 21-amino-acid fragment is produced. This contains 12 amino acids of the peptide which is cleaved off by the T4 prohead protease during head maturation (19); the remaining 9 amino acids are changed by frame shift. The third mutation, 68*fs*mlu, makes a long fragment of 89 amino acids (Fig. 1c).

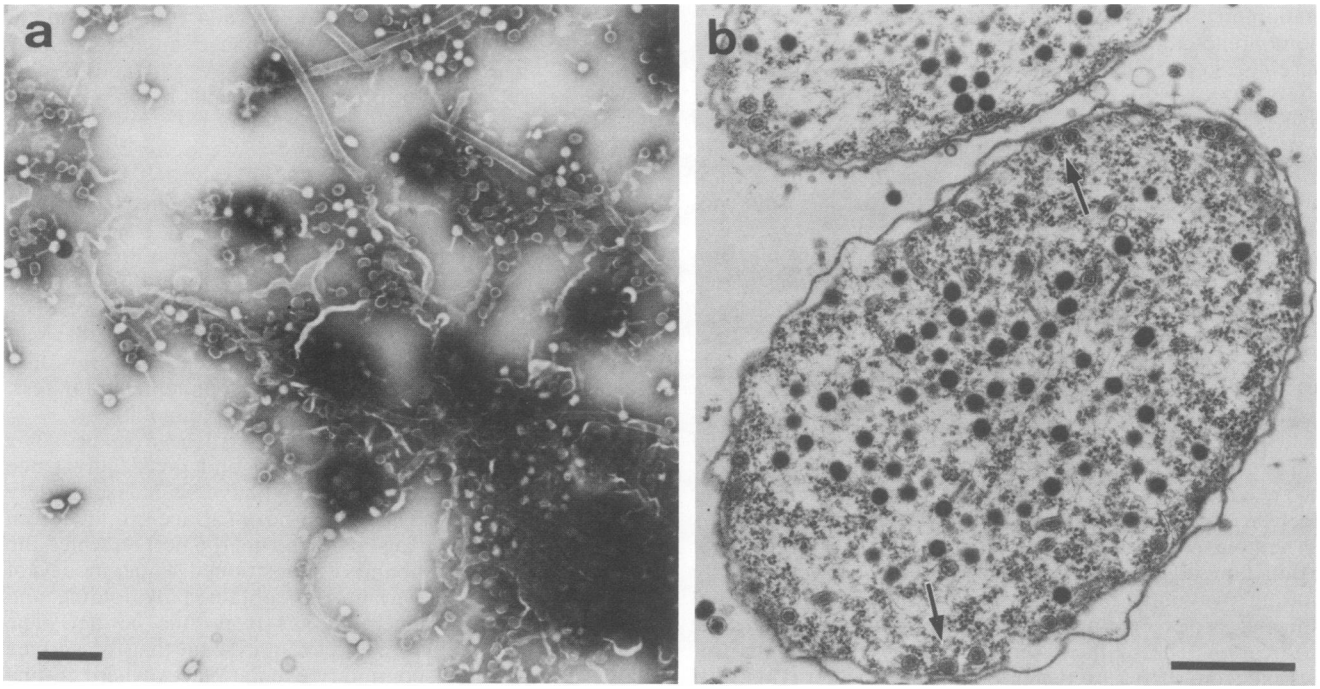

FIG. 2. Electron micrographs of 68*fs*xho-infected cells. (a) In situ lysis of a culture of *E. coli* B infected at 2×10^8 cells per ml at a multiplicity of infection of 5, superinfected 6 min later with the same number of phages, and further incubated for 45 min at 37°C. Long tubular structures (polyheads) and mature phages can be distinguished. (b) Thin section of a cell infected as in panel a but grown for 60 min after infection. The arrows point to some membrane-bound proheads. Bars, 0.5 μm.

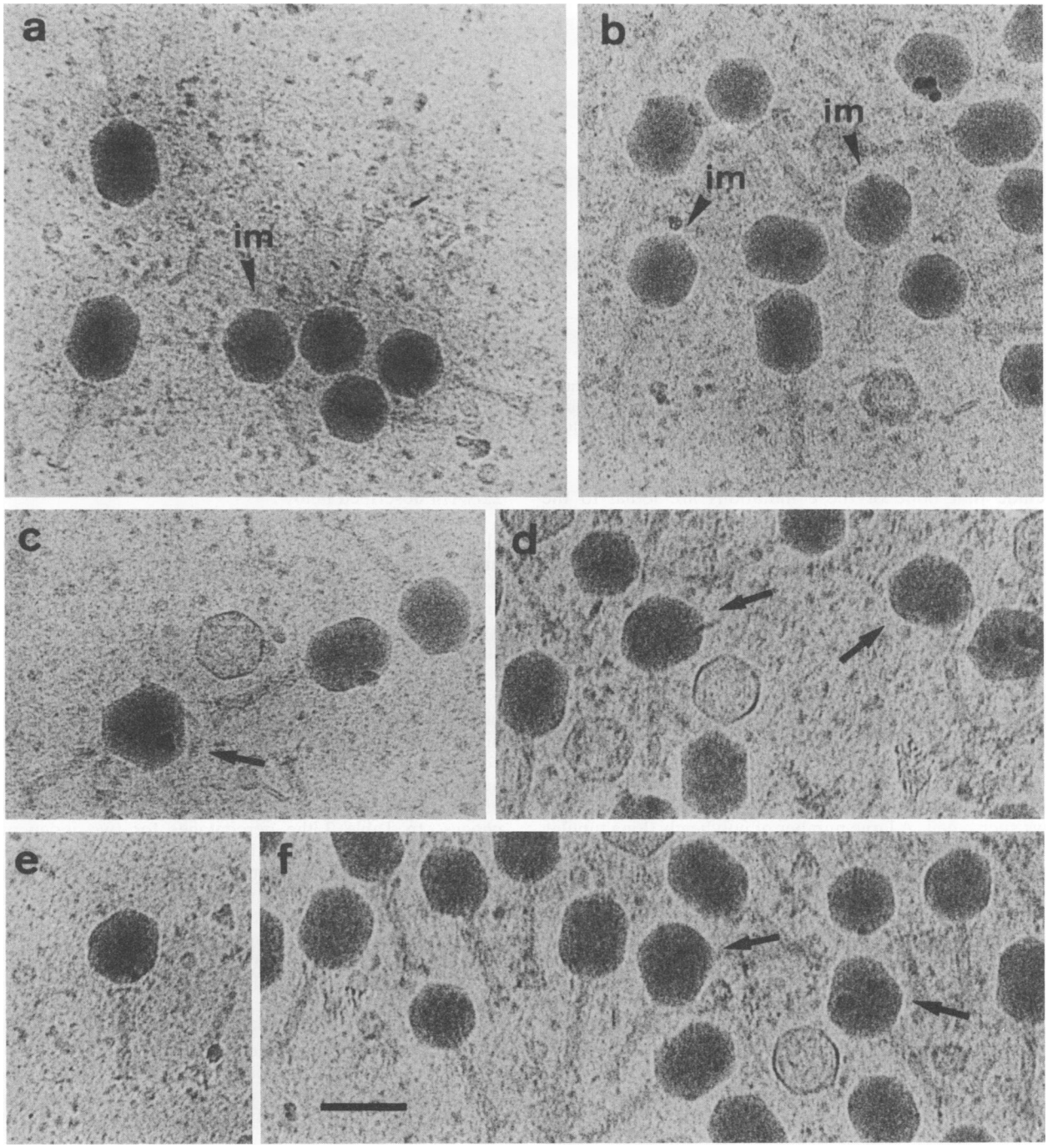

FIG. 3. Electron micrographs of frozen hydrated 68*del*a phages. A crude lysate of phage-infected cells was used. In panels a and b, members of the three length classes of isometric, intermediate, and prolate phages are clearly distinguishable. The arrowheads labeled "im" point to intermediate-length particles. The arrow in panel c indicates a biprolate particle; panels d, e, and f (arrows) show intermediate-length particles with a protrusion on one side and different tail attachment vertices. Bar, 100 nm.

It is not known whether cleavage still occurs during maturation. It is interesting that the fragment is not recognized by immunoblot electrophoresis (8, 34). In this fragment the basic carboxy-terminal part of the native gene product is deleted. These three mutations were recombined back to the phage genome to give mutants T4 68*fs*xho, 68*fs*mlu, and 68*del*a. Bacteria carrying pTV44 with the corresponding mutation in gene 68 were infected with *ts* mutants in each of the neighboring genes 20 and 21, and progeny phages were plated and grown at 42°C (21, 39). In all cases the frequencies of double recombinants were comparable to the frequencies obtained with the wild-type plasmid. Control experiments showed that mutations on the plasmid which are lethal to the phage (e.g. 67*am*K1 or 21*ts*N8) lower the rescue frequency by a factor of 10 (results not shown). Single plaques from these recombination experiments were grown up and tested for synthesis of gp68 with antibodies. Phage lysates containing no gp68 were then chosen. From these observations we

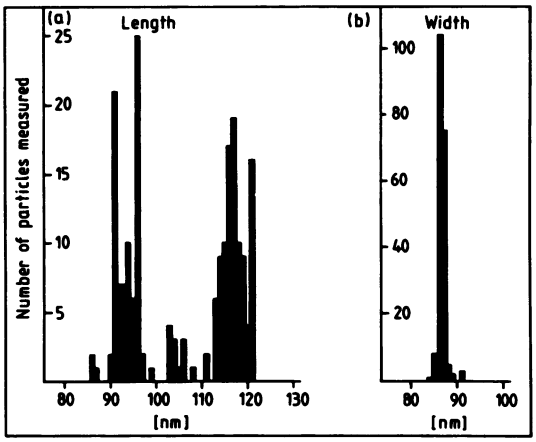

FIG. 4. Length and width distributions of 68*del*a frozen hydrated phages. (a) Head length measurements. The three peaks of length represent the isometric, intermediate, and prolate sizes. A total of 200 particles were measured. (b) Head width measurements.

conclude that none of these mutations are lethal to the phage.

Phenotype of mutants with mutations in gene 68. The burst sizes of the three mutants were compared with that of the wild type. The results are summarized in Table 1. As can be seen, all three mutants produce about the same fraction (20 to 25%) of infective particles compared with wild-type-infected cells. These burst size experiments suggest that a large fraction of structural phage proteins are not assembled into infective phage particles, but are used for noninfective aberrant structures. We observed cells infected with the mutant 68*fs*xho under an electron microscope. A liquid culture of infected *E. coli* B was treated with OsO_4 and lysed in situ on an electron microscope grid (16). The content of single infected cells remains in a confined area. Figure 2a shows such a cell. A large number of polyheads (long tubular structures) and phages with different head lengths and shapes are observed. In thin sections of these cells, black particles (mature DNA-containing heads), polyheads, and also a number of membrane-attached proheads can be observed (Fig. 2b). We also found some aggregates in these cells, which are likely to contain precipitated phage protein ("lumps").

Mature phages (i.e., with packaged DNA) were observed by negative staining to quantitate the classes of particles with clearly distinguishable shapes. In Table 2 the percentages of different head shapes are given. The two mutants 68*del*a and 68*fs*xho both produce about the same number of isometric (petite) and normal prolate particles, indicating that the fragment of 68*fs*xho does not influence length determination. In 68*fs*mlu, however, only half the number of isometric particles are formed when compared with the two other mutants. Possibly the long protein fragment produced by this mutation is partially active.

We wanted to know the exact shapes of the particles produced when gp68 is missing. The shapes and dimensions of the 68*del*a mutant particles were carefully determined by using frozen hydrated specimens (2). In this method, the particles in suspension are trapped within a vitrified ice layer and can be observed unstained. With other methods it is extremely difficult to measure exactly the length and width of a particle because of contraction and deformation associated with the wrapping phenomenon during drying (17). In Fig. 3a and b three length classes of particles can clearly be distinguished: isometrics, intermediates, and normal-length phages. We have measured 200 particles to get a length and width distribution. For particles with normal width, the results are shown in Fig. 4 and confirm the visual observation of three length classes. There may be a class of particles that are a little longer (about 4 to 6 nm) than the normal prolate phages; such particles had also been observed by Mosig et al. (26) in mutants with mutations in gene 23. In 68^- lysates many particles are found which differ not only in length but also in width. We found at least two different kinds of such aberrant particles in frozen hydrated specimens (Fig. 3c to f). One sort of particle (Fig. 3c) is probably identical with the previously described biprolate (5), which is found very rarely in wild-type infections. It can be described as a prolate particle which protrudes on one side. Figure 3d to f shows other aberrant particles. They have an intermediate length and also protrude on one side. Particles of a given head shape are found with different tail attachment sites. In lysates of the mutant 68*del*a, large numbers of double-tailed phages are also found. The morphology of 68*del*a double-tailed phages is indistinguishable from that of multitailed phages found in permissive lysates of the mutant 22*ts*A74 described below.

Form variation of phages in the mutant 22*ts*A74. Paulson et al. (29) described conditions under which a *ts* mutant in the major scaffolding core protein, gp22, produces large numbers of particles with altered width. Some of these particles are shown in Fig. 5. These were prepared either as frozen hydrated material or by a form-preserving type of negative stain (see Materials and Methods). We interpret the altered width in Fig. 5a to c as protrusions of both sides of the particle (triprolate), whereas the biprolate particle (Fig. 5g) protrudes on one side only. There are also other examples of different head shapes. Figure 5d shows a particle which may be isometric with the dimensions of the length of the prolate head. Interestingly, in our experiments, the 22*ts*A74 mutant produced a high percentage of double- and multitailed phages. In Table 3 the percentages for two independent experiments are shown. About two-thirds of all particles have two or more (up to four) tails. We also found that the number of tails is reduced during purification (pelleting or sucrose gradient centrifugation). A quantitative analysis of this phenomenon is also given in Table 3.

Models of phage heads of different sizes and shapes. We have built paper models of the various shapes of the T4 head that we observed. The models were constructed according to the principles described in Materials and Methods and are shown in Fig. 6A to G. We found at least seven distinct sizes and shapes. Table 4 describes the structure of these models in terms of the number (*n*) and the type (*T*, *Q*) of triangles used to build them. The type of triangles used is either

TABLE 3. Occurrence of multitailed phages in 22*ts*A74 lysates[a]

No. of tails	% of phages in following expt:		
	Expt 1[b]	Expt 2[c] (unpurified)	Expt 2[d] (sucrose gradient purified)
1	24.6	33.7	62.9
2	49.1	44.0	26.4
3	26.0	22.4	10.6
4	0.3	0.1	

[a] Phage lysates were prepared as described by Paulson et al. (29) (method B).
[b] A total of 903 particles were counted.
[c] A total of 769 particles were counted.
[d] A total of 564 particles were counted.

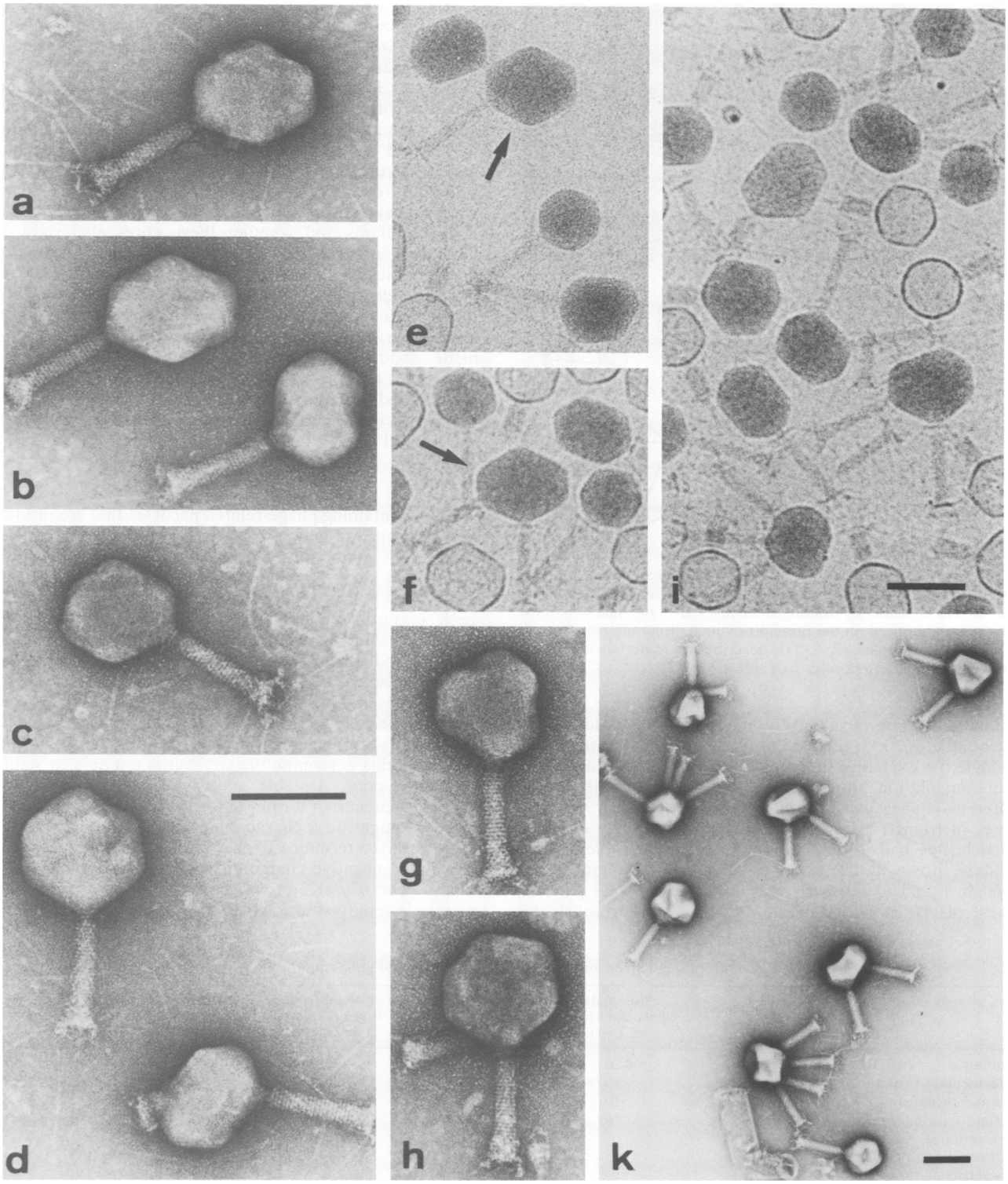

FIG. 5. Electron micrographs of 22*ts*A74 mature phages. The particles were sucrose gradient purified and then observed as frozen hydrated material (panels e, f, and i) or by the form-preserving method of negative stain after being prefixed in uranyl acetate (panels a to d, g, h, and k). The arrows point to particles wider than normal. Panel k shows some of the multitailed phages. Magnifications: a, b, c, g, and h, same as d; e and f, same as i. Bars, 100 nm.

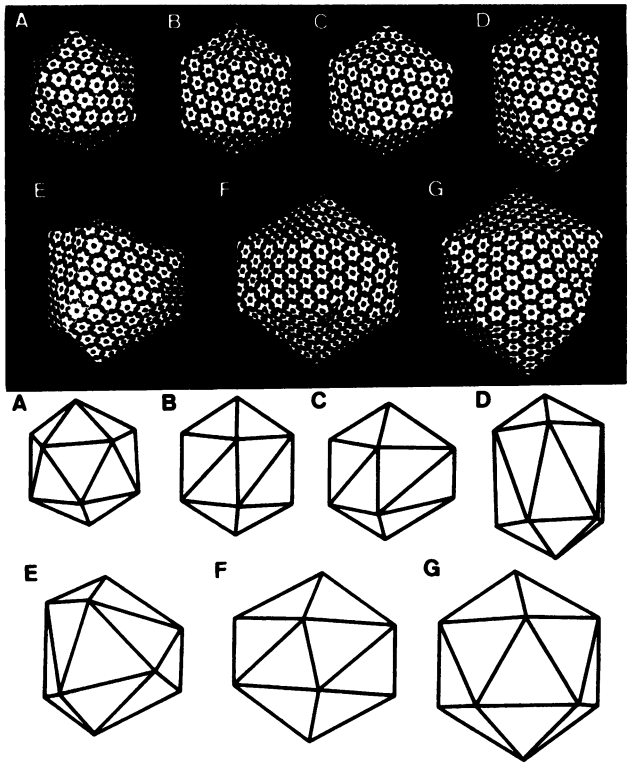

FIG. 6. Paper models and schematic drawings of aberrant head structures based on electron micrographs such as those shown in Fig. 3 and 5 made by folding a hexagonal plane net. All these polyhedra are based on the principles which direct the construction of icosahedral viruses (7, 6, 11), described in Materials and Methods. The capital letters refer to Table 4.

equilateral (T) or irregular (Q), and their size is described by the number $3T$ or $3Q$ of protein subunits contained in a given triangle. As explained in Materials and Methods, T and Q are the triangulation numbers. Interestingly, six of the seven different shapes can be built by using only four different types of triangles. For the intermediate, laterally extruded particle, we had to use additional triangles (Table 4). The models shown fit best with the electron micrographs, although T and Q numbers may differ in the real particle. These results show that the newly observed aberrant shapes can be explained by the same basic rules which describe particles of normal shapes.

Mutants with double mutations in gene 68 and other head genes. Since the prohead contains 200 to 300 molecules of gp68 (27), we wanted to know whether the scaffolding core in 68^- proheads is morphologically distinguishable from normal cores. To observe proheads without gp68 we combined 68*fs*xho with 21*ts*N8. Mutations in gene 21 block head maturation at the prohead level. The particles accumulated by $21^- \cdot 68^-$ are shown in Fig. 7a. Obviously these proheads have different sizes, but no difference in morphology or staining properties can be seen. We then investigated whether naked scaffolding cores can be found in $23^- \cdot 68^-$ double mutants and whether these cores also show size variation. In the double mutant 23*am*H11 · 68*fs*xho, only very few (less than 10% of the number found in 23*am*H11-infected cells) naked scaffolding cores were found. A few of these particles are shown in Fig. 7b. The small number of observable particles does not allow any conclusion to be made about the shape and length of these cores. In 23*am*H11 · 68*fs*mlu no naked cores were found at all. We also studied the double mutant 67*am*K1 · 68*fs*xho. In infections with these mutants no proheads but only polyheads were found (Fig. 7c).

DISCUSSION

DNA containing phage-related particles that are produced in the absence of gp68 show a high percentage of abnormal shapes, an abnormal number of tails, and different tail attachment sites. However, a fraction of normal, infective phages are still produced, confirming the observation that gp68 is only semiessential for the virus. One mutant (68*fs*mlu), which makes a protein fragment of 89 amino acids, is indistinguishable from the deletion mutant 68*del*a (12 amino acids) by its burst size; it is also unable to form naked cores in the absence of the shell protein. However, in 68*fs*mlu the percentage of isometric particles produced is twofold lower. This suggests that the fragment of 68*fs*mlu actively helps determine the size but is not able to stabilize the naked core. A stable, naked core seems not to be a necessary precursor for phage formation. Failure to stabilize the core might be a charge effect due to the missing, very basic carboxy terminus of the mutated protein (19 positive and only 1 negative charge). This is reminiscent of a mutation in gene 67*am*K2 in which the entire acidic part of the protein is removed and which also does not form a stable,

TABLE 4. Different head sizes and shapes found in gp22 and gp68 mutant phage infections[a]

Name	Paper model (Fig. 6)	No. (n_{13}) of equilateral triangles of $T = 13$	No. (n_{27}) of equilateral triangles of $T = 27$	No. (q_{15}) of irregular triangles of $Q = 15$	No. (q_{21}) of irregular triangles of $Q = 21$	No. of unit triangles	No. of subunits, S[b]
Isometric	A	20				260	780
Intermediate prolate[c]	B	10		10		280	840
Normal prolate	D	10			10	340	1,020
Prolate with lateral extrusion (biprolate)	E	6	2		12	384	1,152
Shortened	F		10		10	480	1,440
Isometric	G		20			540	1,620

[a] T and Q numbers are those which were used for model building. From these values, the number of subunits was calculated.

[b] $S = 60\left(\frac{n_{13}}{20}13 + \frac{n_{27}}{20}27 + \frac{q_{15}}{20}15 + \frac{q_{21}}{20}21\right) = 60\sum_{T,Q}\left(\frac{n_T}{20}T + \frac{n_Q}{20}Q\right)$. For isometric, $S = 60T$. For prolate, $S = 60(T/2 + Q/2) = 30(T + Q)$.

[c] For the intermediate heads with lateral extrusion (model C in Fig. 6), other triangles were used.

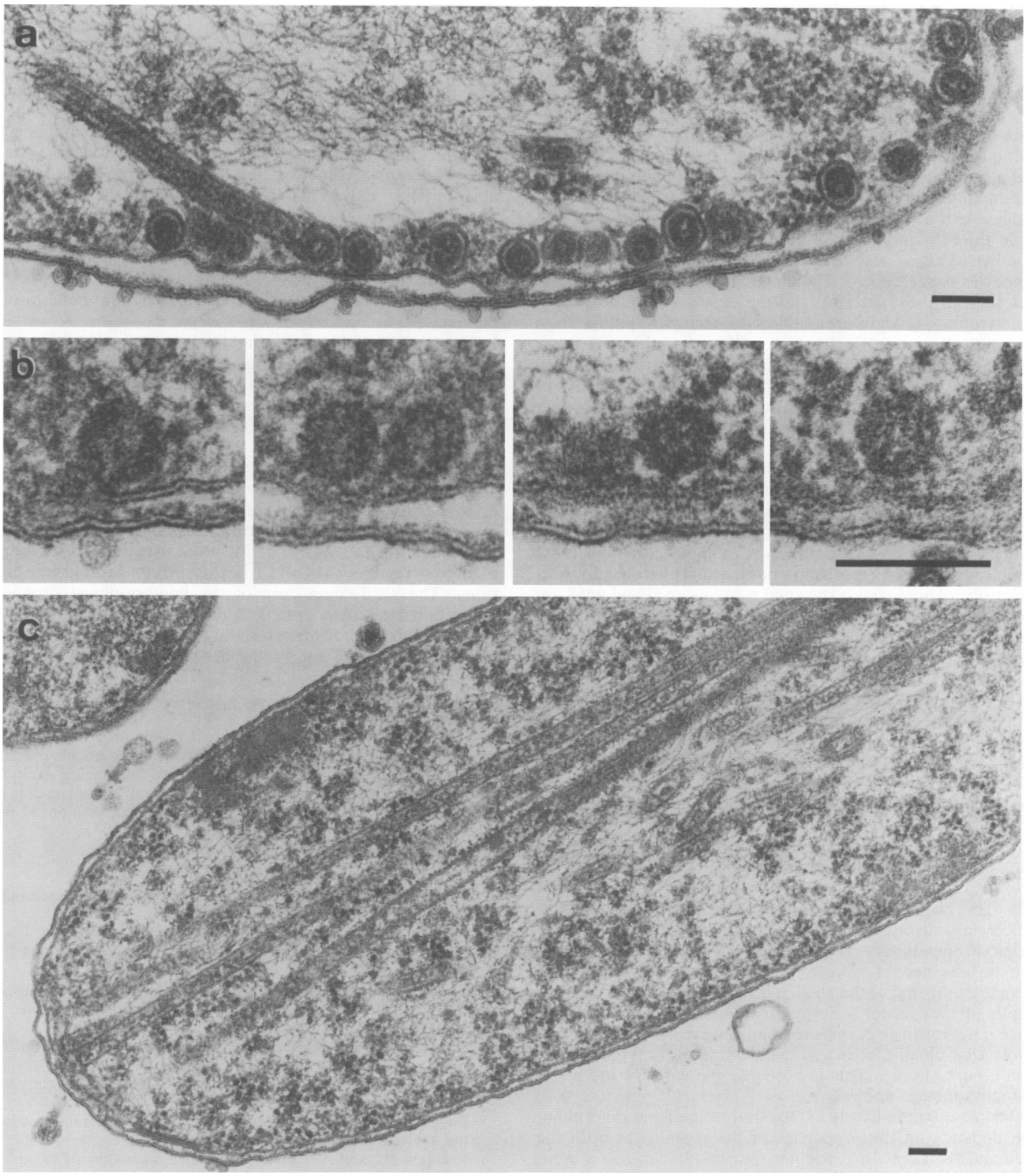

FIG. 7. Electron micrographs of double mutants with mutations in gene 68 and other head genes. *E. coli* B cells were grown to a density of 2×10^8 cells per ml and then infected and superinfected 6 min later at a multiplicity of infection of 5 each time. The culture was further incubated for 60 min at 37°C (or 41°C for 21*ts*N8 · 68*fs*xho). Thin sections of cells infected with 21*ts*N8 · 68*fs*xho (a), 23*am*H11 · 68*fs*xho (b), and 67*am*K1 · 68*fs*xho (c) are shown. Except for the form variation, the proheads in panel a are indistinguishable in morphology and staining properties from 21^- proheads. In panel b, some of the very few naked scaffolding cores formed in 23*am*H11 · 68*fs*xho infections are shown. In panel c, polyheads (long tubular structures) can be seen. Bars, 100 nm.

naked core (20). In addition, 67*am*K2 is, like 68^-, semiessential and shows form variation.

The much better form preservation of frozen hydrated material enabled us to describe several classes of aberrant head shapes by using electron microscopy. For one core protein mutant we could demonstrate heads of intermediate length. Previously, intermediate-sized phage particles had been found only in shell protein mutants, together with isometric variants (12). They were infective, although they had a reduced length of the genome (9, 26). We also found intermediate-length particles with a protrusion. Prolate phages with a protrusion (biprolates) have been known for some time (5) and seem to be formed only by core protein mutants. This is also true for the newly described large isometric particle ($T = 27$) and its shortened version. The fact that all these variants can be described by polyhedra built from a few different sorts of triangles points to a common aberration in the core structure underlying these defects. Knowing nothing precise about the structure of the core, we cannot even speculate about the molecular basis of these aberrations. Since only mutations in genes encoding core proteins produce particles of aberrant width and with protrusions, it is possible that the core can also assume different shapes when one of its protein components is missing or conformationally wrong. Another possibility is an active misguiding of the shell by the core during concomitant growth of core and shell, giving rise to the protrusions. There is some evidence for concomitant core and shell assembly: $21^- \cdot 68^-$ proheads have a morphologically normal prohead core, but if the shell proteins gp23 and gp68 are both absent, no or only very few cores are found in thin sections. We think that the 68^- core is stabilized by gp23 and, contrary to cores containing gp68, cannot exist without the shell.

We now have several mutations in core protein genes which produce isometric phages and proheads. None of them produces enough naked cores for us to decide whether there is already a form variation at the core level. These observations are all in agreement with the idea that the prolate form represents the only relatively stable form and length of a naked scaffolding core. Thus, the core inside the isometric prohead would be an incomplete structure. We think that the intrinsic curvature of gp23 (33) favors a closure into an isometric head when an incomplete core is present (36). This would happen, e.g., in the 67*am*K1 mutant, in which only disorganized cores are seen in the mainly isometric proheads (20). A weak core structure, due to mutation or absence of a core protein, would then result in premature closing of the shell at an isometric or intermediate length of the particle. Premature closing would also take place if the intrinsic curvature of gp23 were increased in such a way that closing at the isometric size was favored, even with a normal core. This is probably the case for the petite (pt) mutations in gp23 (9).

Our results definitively establish that the form determination depends on the properties of the proteins of both the shell and the core. In particular, our results suggest a more passive role of the core in length determination, whereas the width seems to depend entirely on the core which guides the nascent shell farther apart than normal, e.g., to form a structure based on $T = 27$. Shell protein mutants have never been found to produce particles of altered width (4).

Besides the differences in head morphology, the frequent occurrence of particles with several tails is striking in the described mutants. The intermediate, laterally extruded particle, e.g., uses at least three different vertices for tail attachment. This probably reflects growth of the prohead at the membrane in three different orientations, again showing the instability and flexibility of the gene 68 defective core. With 22*ts*A74, our growth conditions result in a quantitative production of multitailed phages (60 to 75%), demonstrating that the core can affect the location and number of tails. Recently descriptions of cores with tails (22) even suggest that the core, with connector but without shell, can mediate tail attachment. We think that the same structural abnormalities which give form variation are also responsible for the attachment of extra tails. The extra-attachment vertices are abnormal and give rise to less strongly bound tails, which are easily lost. The additional site might be normal initiation structures for core assembly, which, owing to abnormal core structures, might be positioned at two or three vertices. These initiation structures would later become head-to-tail connectors.

Giant bacteriophages frequently have tails at both ends. Although it is known that giants are able to inject their multiple genome (9), nothing is known about both tails being functional. It would also be interesting to study the aberrant and multitailed particles described in this paper in terms of this phenomenon. Adequate experiments have still to be developed.

Future electron microscopy studies and biochemical cross-linking studies should allow us to learn more about the prohead core structure. In vitro-produced mutations in core genes should allow one to define more precisely which parts of the proteins are involved in the protein-protein interactions. The scaffolding core of the bacteriophage prohead might thus become a suitable specimen with which to study the mechanisms of form determination at the molecular level of protein structure and function.

ACKNOWLEDGMENTS

We thank Toni Völker and Christian Sengstag for gifts of materials used in this work and Marlies Zoller for photographical assistance. We also thank Thomas A. Bickle, Eric Carlemalm, Andreas Kuhn, and Rolf Stalder for helpful discussions and critical reading of the manuscript and Regula Niederhauser for preparation of the typescript.

LITERATURE CITED

1. **Adams, M. H.** 1959. Bacteriophages, p. 446. Interscience Publishers, Inc., New York.
2. **Adrian, M., J. Dubochet, J. Lepault, and A. W. McDowall.** 1984. Cryo-electron microscopy of viruses. Nature (London) **308**:32–36.
3. **Black, L. W., and D. T. Brown.** 1976. Head morphologies in bacteriophage T4 head and internal protein mutant infections. J. Virol. **17**:894–905.
4. **Black, L. W., and M. K. Showe.** 1983. Morphogenesis of the T4 head, p. 219–245. *In* C. K. Matthews, E. M. Kutter, G. Mosig, and P. B. Berget (ed.), Bacteriophage T4. American Society for Microbiology, Washington, D.C.
5. **Boy de la Tour, E., and E. Kellenberger.** 1965. Aberrant forms of the T-even phage head. Virology **27**:222–225.
6. **Branton, D., and A. Klug.** 1975. Capsid geometry of bacteriophage T2: freeze-etching study. J. Mol. Biol. **92**:559–565.
7. **Caspar, D. L. D., and A. Klug.** 1962. Physical principles in the construction of regular viruses. Cold Spring Harbor Symp. Quant. Biol. **27**:1–24.
8. **De Blas, A. L., and H. M. Cherwinski.** 1983. Detection of antigens on nitrocellulose paper immunoblots with monoclonal antibodies. Anal. Biochem. **133**:214–219.
9. **Doerman, A. H., F. A. Eiserling, and L. Boehner.** 1973. Genetic control of capsid length in bacteriophage T4. I. Isolation and preliminary description of four new mutants. J. Virol. **12**:374–

385.
10. **Eiserling, F. A.** 1979. Bacteriophage structure, p. 543–580. *In* H. Fraenkel-Conrat and R. R. Wagner (ed.), Comprehensive virology, vol. 13. Plenum Publishing Corp., New York.
11. **Eiserling, F. A.** 1983. Structure of the T4 virion, p. 11–24. *In* C. K. Matthews, E. M. Kutter, G. Mosig, and P. B. Berget (ed.), Bacteriophage T4. American Society for Microbiology, Washington, D.C.
12. **Eiserling, F. A., E. P. Geiduschek, R. H. Epstein, and E. J. Metter.** 1970. Capsid size and deoxyribonucleic acid length: the petite variant of bacteriophage T4. J. Virol. **6**:865–876.
13. **Engel, A., R. Van Driel, and R. Driedonks.** 1982. A proposed structure of the prolate phage T4 prehead core. An electron microscopic study. J. Ultrastruct. Res. **80**:12–22.
14. **Epstein, R. H., A. Bolle, C. M. Steinberg, E. Kellenberger, E. Boy de la Tour, R. Chevalley, R. S. Edgar, M. Susman, G. H. Denhardt, and A. Lielausis.** 1963. Physiological studies of conditional lethal mutants of bacteriophage T4D. Cold Spring Harbor Symp. Quant. Biol. **28**:375–394.
15. **Kellenberger, E.** 1984. Form determination of subcellular biological structures as for example viruses. Helv. Phys. Acta **57**: 188–201.
16. **Kellenberger, E., F. A. Eiserling, and E. Boy de la Tour.** 1968. Studies on the morphopoiesis of the head of phage T-even. III. The cores of head-related structures. J. Ultrastruct. Res. **21**: 335–360.
17. **Kellenberger, E., M. Häner, and M. Wurtz.** 1982. The wrapping phenomenon in air-dried and negatively stained preparations. Ultramicroscopy **9**:139–150.
18. **Keller, B., and T. A. Bickle.** 1986. The nucleotide sequence of gene 21 of bacteriophage T4 coding for the prohead protease. Gene **49**:245–251.
19. **Keller, B., E. Kellenberger, T. A. Bickle, and A. Tsugita.** 1985. Determination of the cleavage site of the phage T4 prohead protease in gene product 68: influence of protein secondary structure on cleavage specifity. J. Mol. Biol. **186**:665–667.
20. **Keller, B., M. Maeder, C. Becker-Laburte, E. Kellenberger, and T. A. Bickle.** 1986. Amber mutants in gene 67 of phage T4: effects on formation and shape determination of the head. J. Mol. Biol. **190**:83–95.
21. **Keller, B., C. Sengstag, E. Kellenberger, and T. A. Bickle.** 1984. Gene 68, a new bacteriophage T4 gene which codes for the 17K prohead core protein, is involved in head size determination. J. Mol. Biol. **179**:415–430.
22. **Kuhn, A., B. Keller, M. Maeder, and F. Traub.** 1987. Prohead core of bacteriophage T4 can act as an intermediate in the T4 head assembly pathway. J. Virol. **61**:113–118.
23. **Laemmli, U. K.** 1970. Cleavage of structural proteins during the assembly of the head of bacteriophage T4. Nature (London) **227**:680–685.
24. **Maniatis, T., E. F. Fritsch, and J. Sambrook.** 1982. Molecular cloning: a laboratory manual, p. 97–148. Cold Spring Harbor Laboratory, Cold Spring Harbor, N.Y.
25. **Messing, J.** 1983. New M13 vectors for cloning. Methods Enzymol. **101**:20–78.
26. **Mosig, G., J. R. Carnighan, J. B. Bibring, R. Cole, H.-G.O. Bock, and S. Bock.** 1972. Coordinate variation in lengths of deoxyribonucleic acid molecules and head lengths in morphological variants of bacteriophage T4. J. Virol. **9**:857–871.
27. **Onorato, L., B. Stirmer, and M. K. Showe.** 1978. Isolation and characterization of bacteriophage T4 mutant preheads. J. Virol. **27**:409–426.
28. **Paulson, J. R., and U. K. Laemmli.** 1977. Morphogenetic core of the bacteriophage T4 head. Structure of the core in polyheads. J. Mol. Biol. **111**:459–485.
29. **Paulson, J. R., S. Lazaroff, and U. K. Laemmli.** 1976. Head length determination in bacteriophage T4: the role of the core protein P22. J. Mol. Biol. **103**:155–174.
30. **Sanger, F., S. Nicklen, and A. R. Coulson.** 1977. DNA sequencing with chain-terminating inhibitors. Proc. Natl. Acad. Sci. USA **74**:5463–5467.
31. **Showe, M. K., and L. W. Black.** 1973. Assembly core of bacteriophage T4: an intermediate in head formation. Nature (London) New Biol. **242**:70–75.
32. **Showe, M. K., and L. Onorato.** 1978. Kinetic factors and form determination of the head of bacteriophage T4. Proc. Natl. Acad. Sci. USA **75**:4165–4169.
33. **Steven, A. C., U. Aebi, and M. K. Showe.** 1976. Folding and capsomere morphology of the P23 surface shell of bacteriophage T4 polyheads from mutants in five different head genes. J. Mol. Biol. **102**:373–407.
34. **Towbin, H., T. Staehelin, and J. Gordon.** 1979. Electrophoretic transfer of proteins from polyacrylamide gels to nitrocellulose sheets: procedure and some applications. Proc. Natl. Acad. Sci. USA **76**:4350–4354.
35. **Traub, F., B. Keller, A. Kuhn, and M. Maeder.** 1984. Isolation of the prohead core of bacteriophage T4 after cross-linking and determination of protein composition. J. Virol. **49**:902–908.
36. **Traub, F., and M. Maeder.** 1984. Formation of the prohead core of bacteriophage T4 in vivo. J. Virol. **49**:892–901.
37. **Van Driel, R., F. Traub, and M. K. Showe.** 1980. Probable localization of the bacteriophage T4 prehead proteinase zymogen in the center of the prehead core. J. Virol. **36**:220–223.
38. **Völker, T. A., J. Gafner, T. A. Bickle, and M. K. Showe.** 1982. Gene 67, a new essential bacteriophage T4 head gene, codes for a prehead core component, PIP. I. Genetic mapping and DNA sequences. J. Mol. Biol. **161**:479–489.
39. **Völker, T. A., A. Kuhn, M. K. Showe, and T. A. Bickle.** 1982. Gene 67, a new essential bacteriophage T4 head gene, codes for a prehead core component, PIP. II. The construction *in vitro* of unconditionally lethal mutants and their maintenance. J. Mol. Biol. **161**:491–504.